Efficient Molybdenum (VI) Modified Zr-MOF Catalyst for Epoxidation of Olefins

Jia Tang,[a] Wenjun Dong,[b] Ge Wang,*[a] Yuze Yao,[a] Leiming Cai,[a] Yi Liu,[a] Xuan Zhao,[a] Jingqi Xu,[a] and Li Tan[a]

[a] School of Materials Science and Engineering, University of Science and Technology Beijing, Beijing 100083, P.R. China
[b] Center for Optoelectronics Materials and Devices, Zhejiang Sci-Tech University, Hangzhou 310018, P.R. China

SUPPORTING INFORMATION

Synthesis of 2-pyridine chloride

2-Pyridine chloride was synthesized according to the literature.[1] Pyridinoic acid (5 g, 40.5 mmol) was suspended in 40 ml toluene at 0°C in N_2 atmosphere in a round-bottom one-neck 100 ml flask equipped with a condenser, a magnetic stirrer, and a condenser. Oxalyl chloride (7.06 ml, 81 mmol) was dropped slowly by syringe, after 1h the ice bath was removed and the reaction was kept overnight at room temperature. The solid was filtered and washed with toluene for 3-4 times and dried in vacuo at room temperature.

Synthesis of $MoO(O_2)_2.2DMF$

10 g MoO_3 and 50 ml 30%H_2O_2 were added in a round-bottom one-neck 100 ml flask and stirred at 40°C for 4h, then 11.2ml DMF was added into the flask, the reaction was kept for 2h at room temperature, after that the filtrate was filtered out from the mixture, stored in the refrigerator for 7days. The precipitated crystals were washed with ethanol several times, dried and preservated. [2-3]

^{1}H NMR

The material (6 mg) was digested in $CDCl_3$ (600 μL) and 40% HF (100 μL) solution by sonication and centrifuged. The supernatant liquid was analyzed by 1H-NMR.

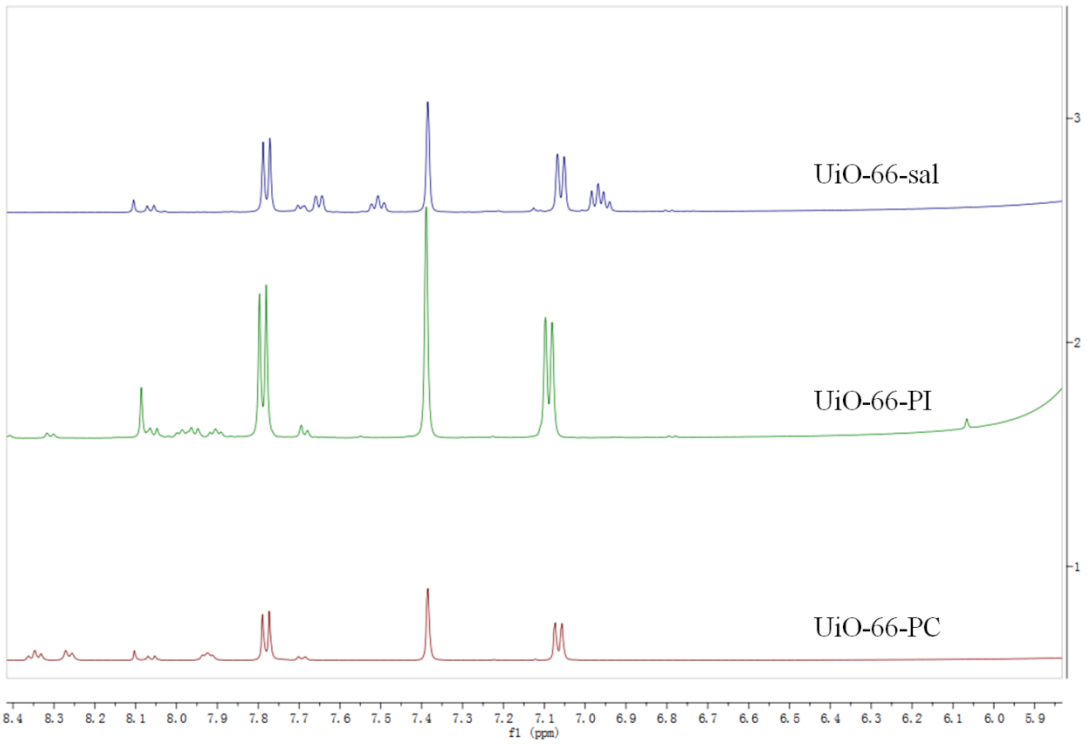

Figure S1.1H NMR spectra of UiO-66(NH_2) modified samples.

FT-IR

Fourier transformed infrared spectra (FT-IR) was recorded by a NICOLET 6700 infrared spectrophotometer with KBr pellet sample.

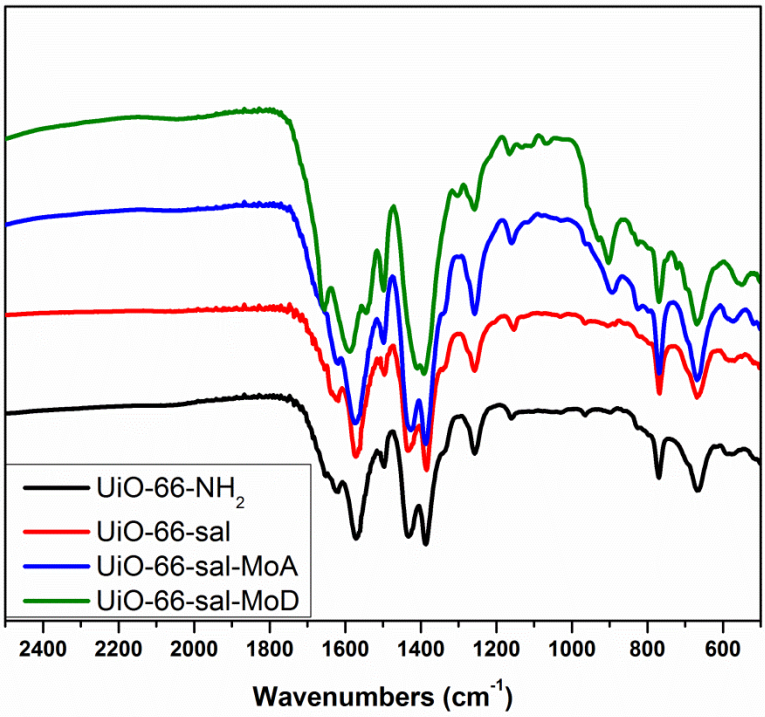

Figure S2.Infrared spectraof UiO-66-NH_2, UiO-66-sal, UiO-66-sal-MoA, UiO-66-sal-MoD.

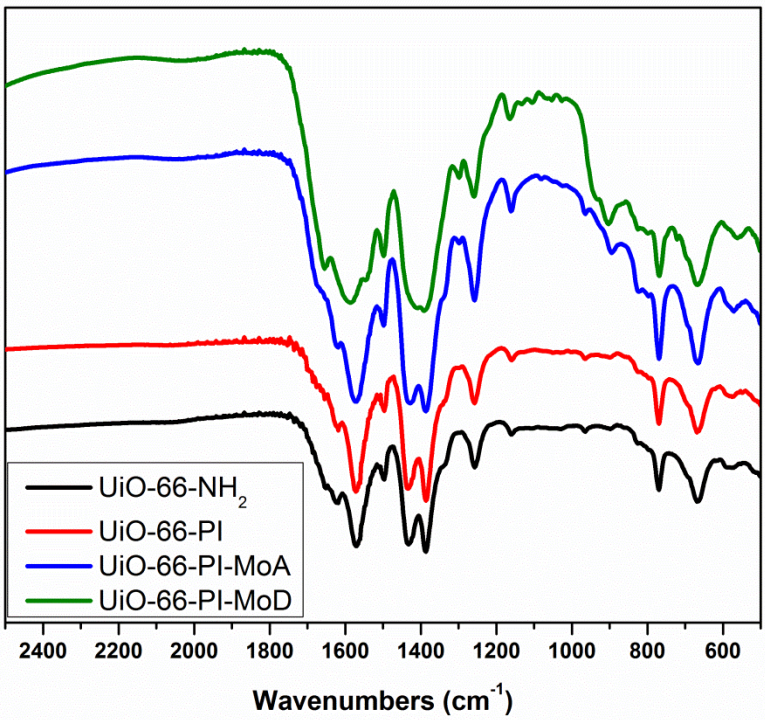

Figure S3.Infrared spectra of UiO-66-NH_2, UiO-66-PI, UiO-66-PI-MoA, UiO-66-PI-MoD.

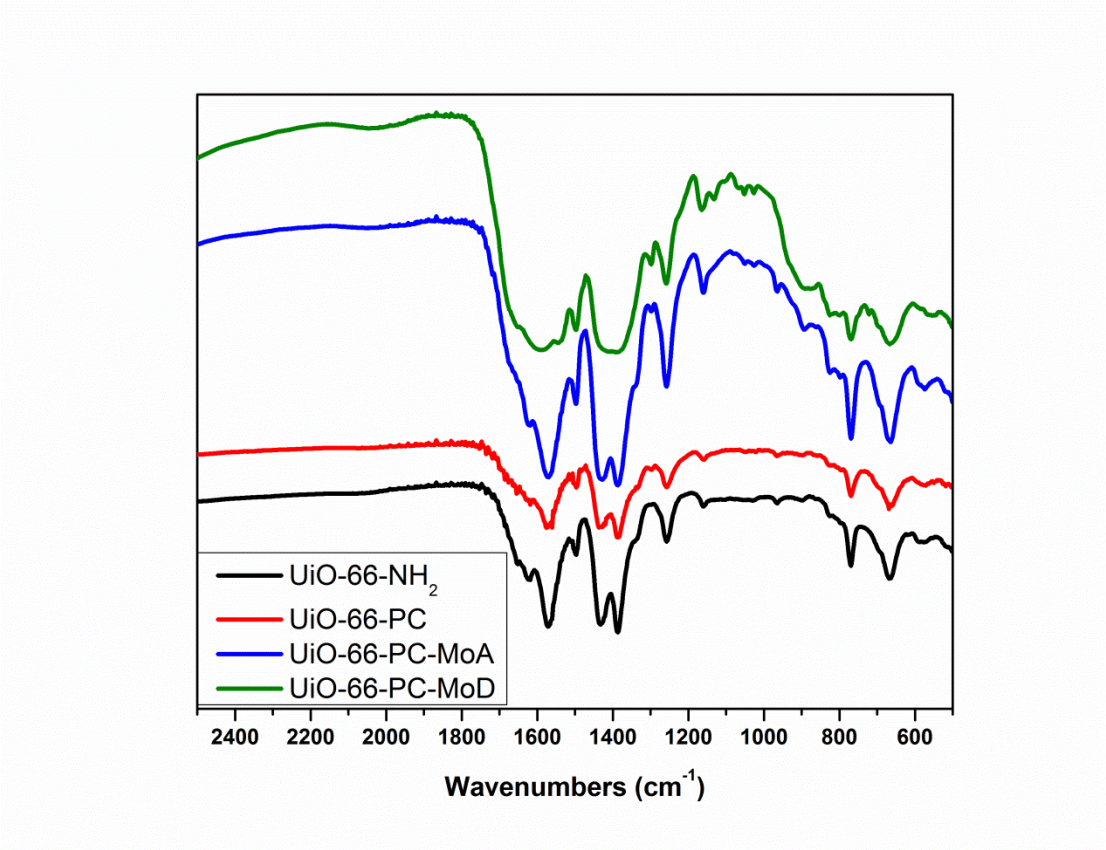

Figure S4.Infrared spectra of UiO-66-NH_2, UiO-66-PC, UiO-66-PC-MoA, UiO-66-PC-MoD.

TGA test

Thermogravimetricanalysis (TG) was conducted with a TGA instrument (Netzsch STA449F) at a heating rate of 10°C/min under an N_2 flow. The specific surface areas were calculated with nitrogen sorption–desorption isotherms using a Micromeritics ASAP 2420 adsorption analyzer.

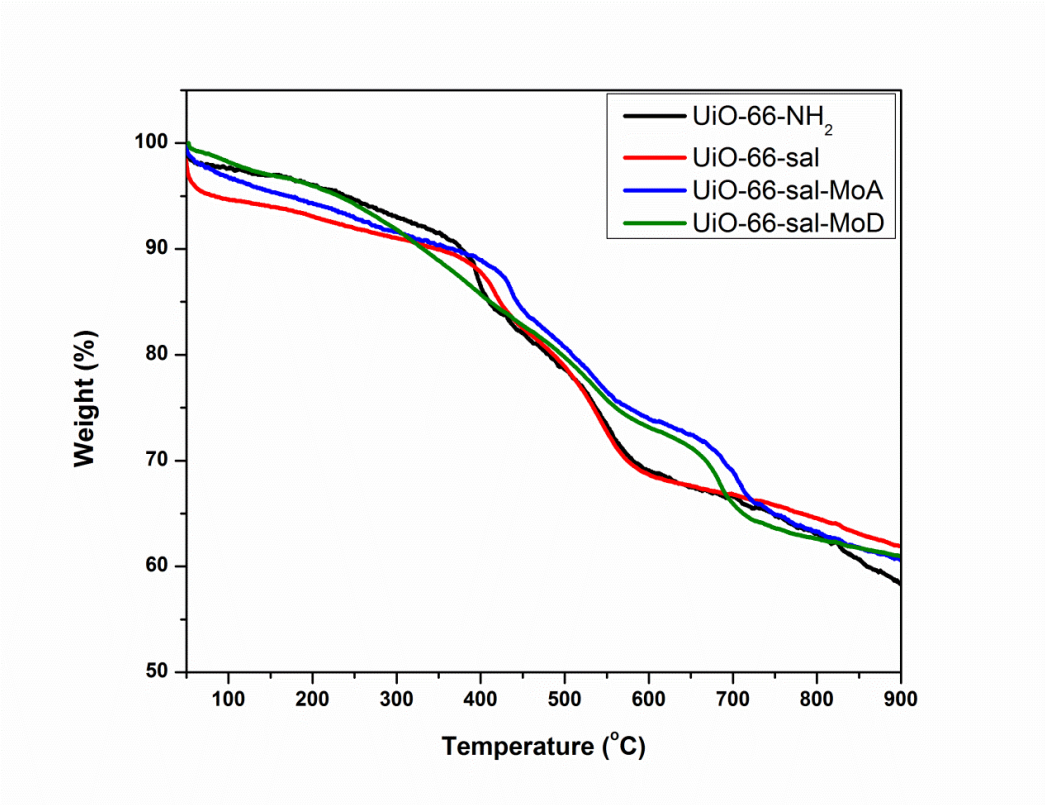

Figure S5.Thermogravimetric analysis of UiO-66-NH_2, UiO-66-sal, UiO-66-sal-MoA, and UiO-66-sal-MoD.

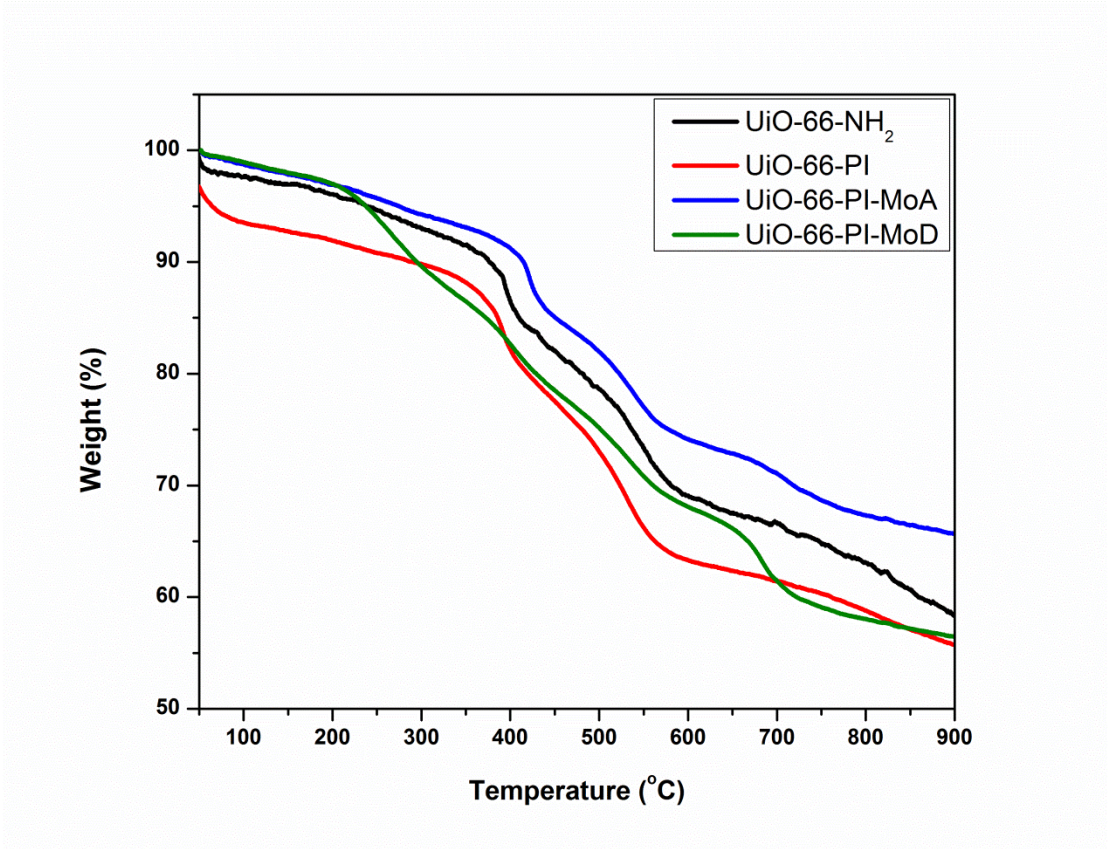

Figure S6.Thermogravimetric analysis of UiO-66-NH_2, UiO-66-PI, UiO-66-PI-MoA, and UiO-66-

PI-MoD

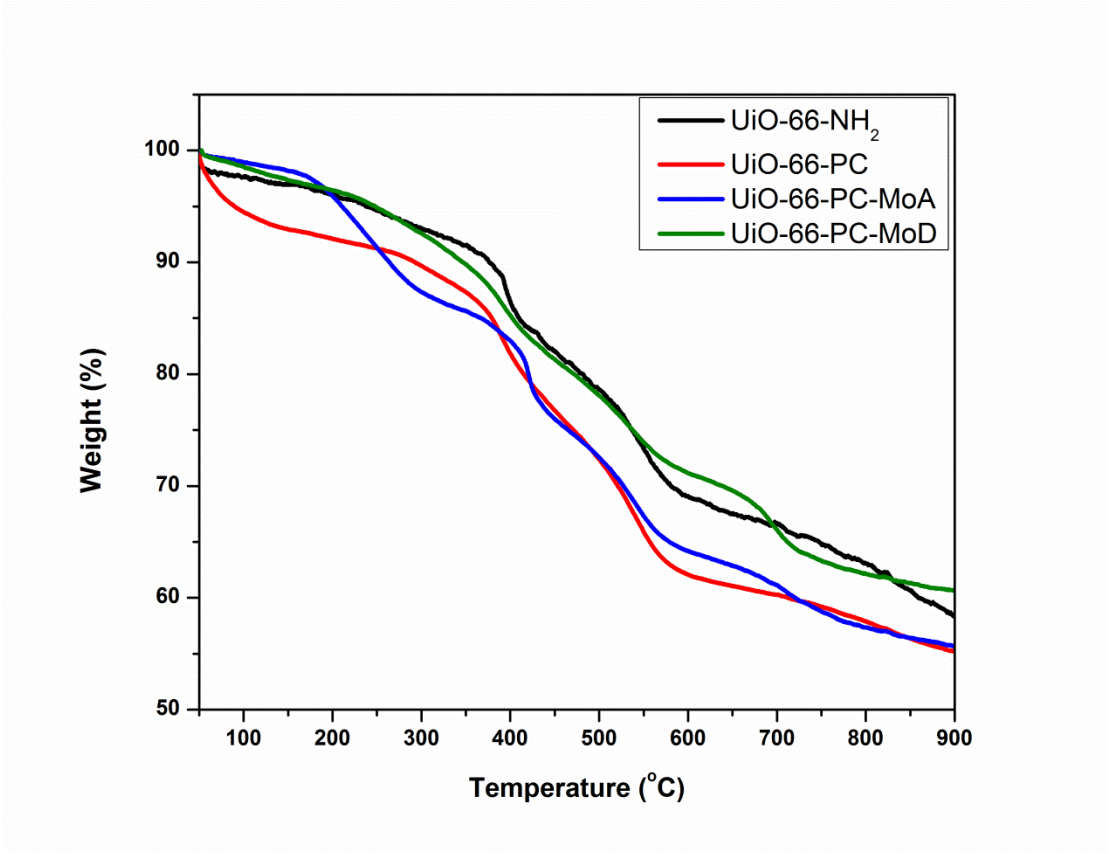

Figure S7.Thermogravimetric analysis of UiO-66-NH_2, UiO-66-PC, UiO-66-PC-MoA, and UiO-66-PC-MoD.

The specific surface areas and nitrogen isotherms measurements

The specific surface areas were calculated with nitrogen sorption–desorption isotherms using a Micromeritics ASAP 2420 adsorption analyzer. The pore size distributions were derived from the adsorption branches of isotherms by using the Barrett–Joyner–Halenda (BJH) model.

Table S1. Surface areas, pore volumes and pore width of the UiO-66 MOFs.

MOF	$S_{BET}(m^2g^{-1})$	$S_{lang}(m^2g^{-1})$	Pore volume(cc/g)	Pore width(nm)
UiO-66-NH_2	1263.6	1337.7	0.600	1.167
UiO-66-NH_2-sal	994.915	1040.4	0.439	0.823
UiO-66-NH_2-PI	1076.706	1126.6	0.522	0.982
UiO-66-NH_2-PC	1003.910	1038.5	0.434	0.863

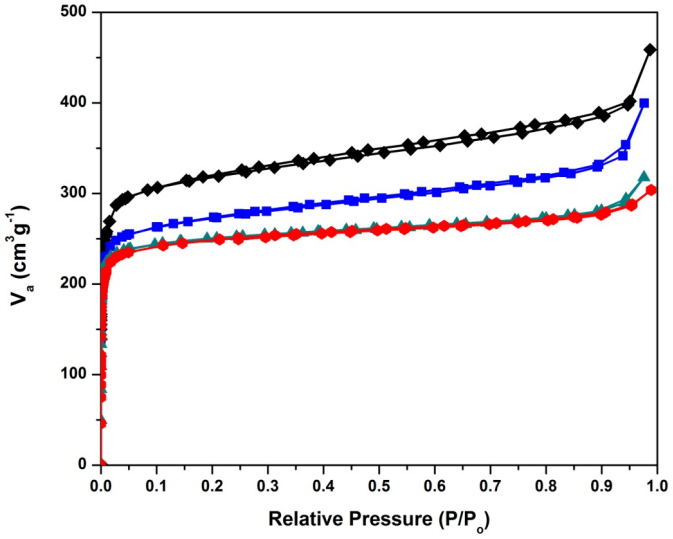

Figure S8.Nitrogen adsorption isotherms at 77 K of the as-synthesized UiO-66(NH_2)(◆), UiO-66-PI(■), UiO-66-PC(▲), UiO-66-sal(●).

Table S2. Surface areas, pore volumes and pore width of the UiO-66 MOFs.

Catalytic Materials	**S_{BET} (m^2/g)**	**S_{lang} (m^2/g)**	**Pore volume (cc/g)**	**ICP (Mo) (wt%)**
UiO-66-sal-MoD	558	587	0.29	15.2
UiO-66-PI-MoD	540	567	0.19	13.1
UiO-66-PC-MoD	674	709	0.11	8.53
UiO-66-sal-MoA	862	893	0.39	8.84
UiO-66-PI-MoA	939	981	0.38	5.03
UiO-66-PC-MoA	893	935	0.31	4.13

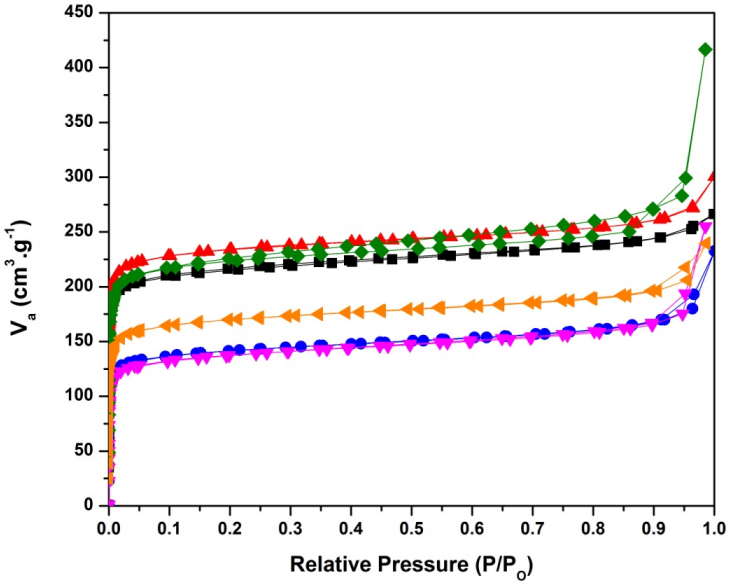

Figure S9.Nitrogen adsorption isotherms at 77 K of the as-synthesized UiO-66-sal-MoA (■), UiO-66-sal-MoD (●), UiO-66-PI-MoA (▲), UiO-66-PI-MoD (▼), UiO-66-PC-MoA (◆), UiO-66-PC-MoD (◀).

XRD

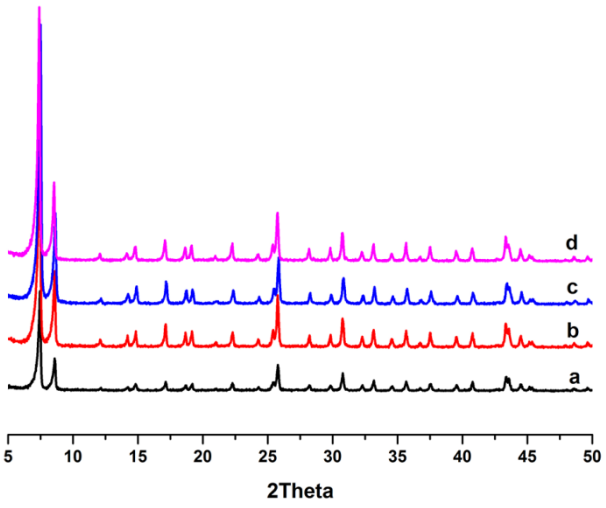

Figure S10.X-ray diffraction patterns for: (a) UiO-66-NH_2; (b) UiO-66-sal; (c) UiO-66-PI; (d) UiO-66-PC.

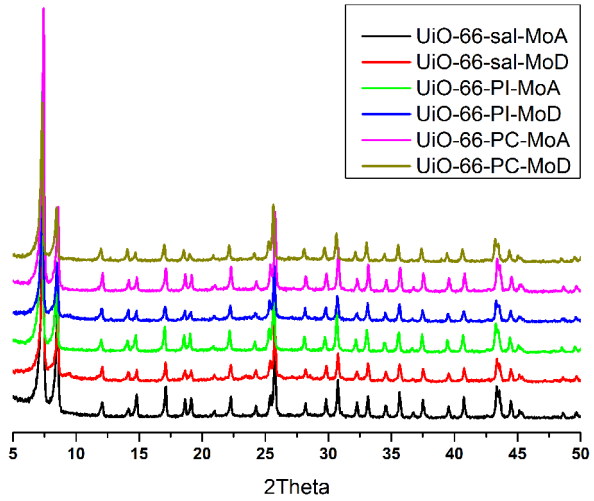

Figure S11.X-ray diffraction patterns for Mo-UiO-66 catalysts.

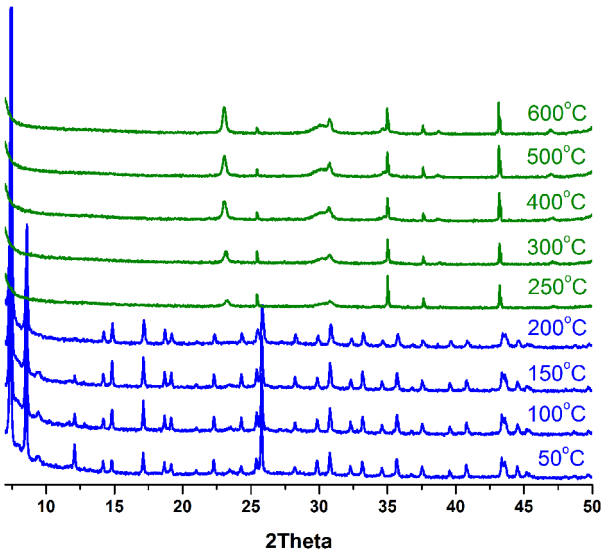

Fig S12.Temperature-dependent powder X-ray diffraction was performed on UiO-66-sal-MoD sample under ambient air.

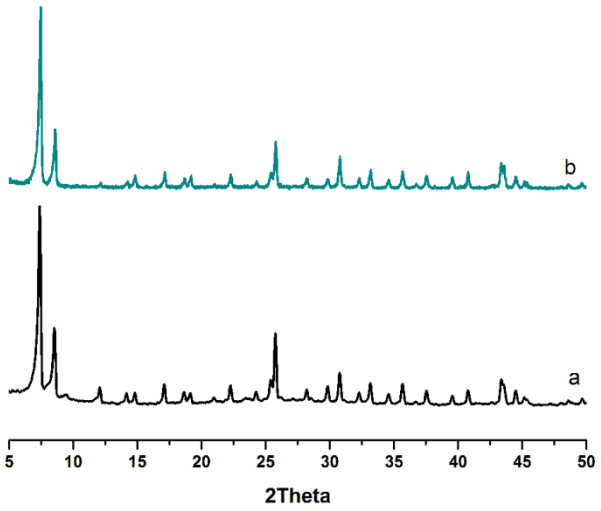

Fig S13.XRPD of UiO-66-sal-MoD (a) fresh and (b) recovered after reaction.

SEM

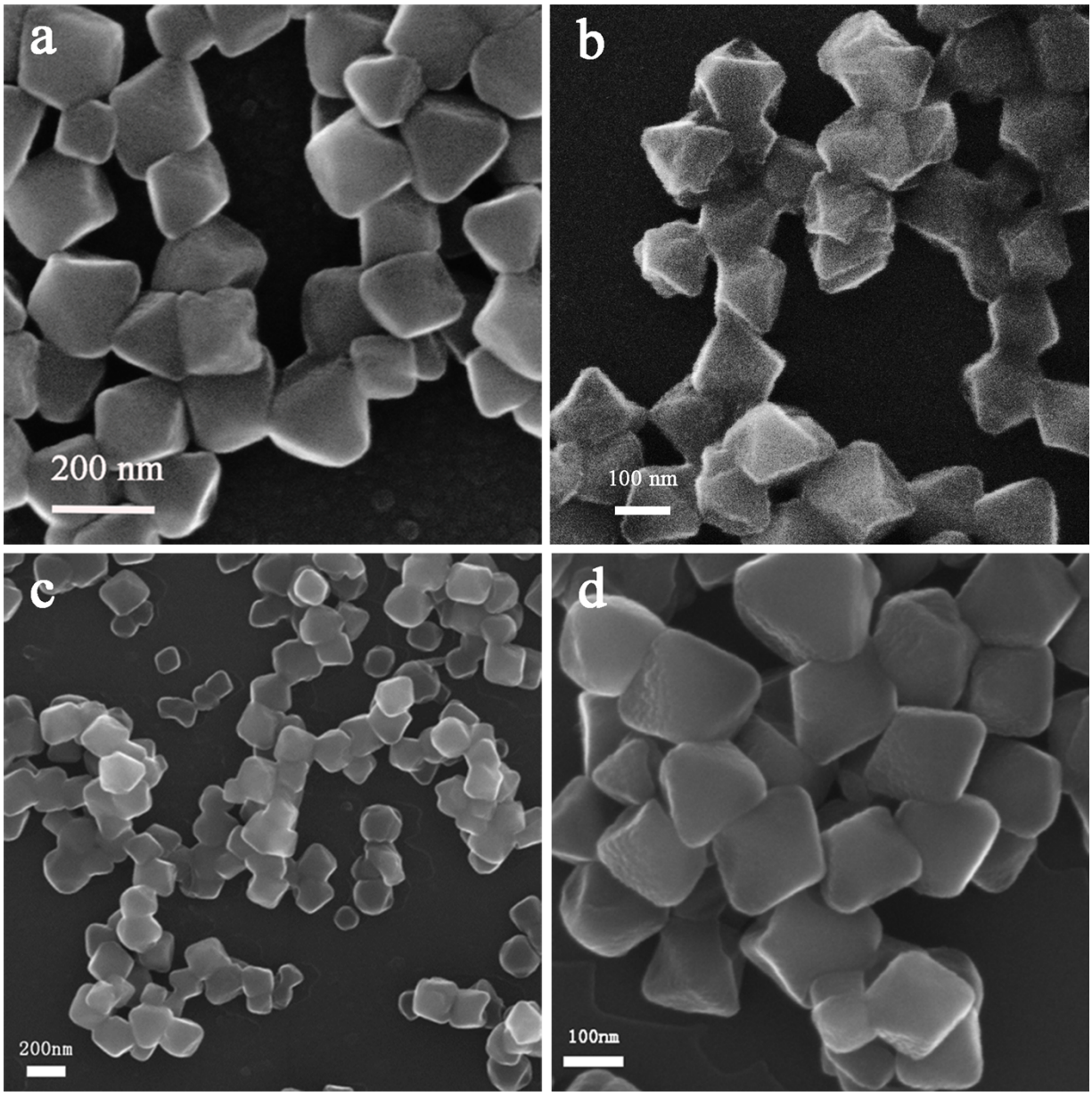

Fig S14.SEM images (a) of UiO-66-NH2, (b) UiO-66-sal, (c) UiO-66-PI and (d) UiO-66-PC.

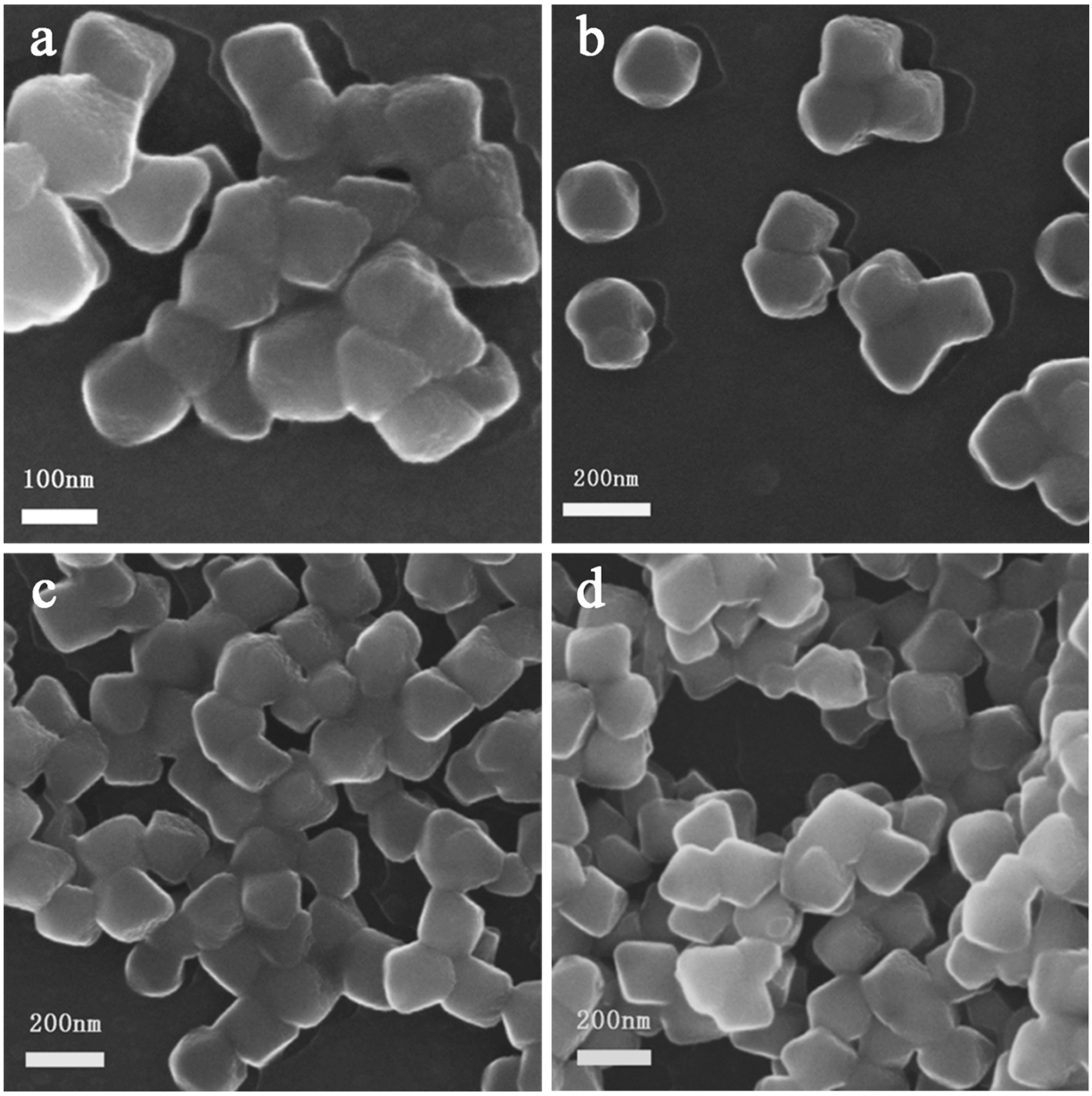

Fig S15.SEM images (a) of UiO-66-sal-MoA, (b) UiO-66-PI-MoD, (c) UiO-66-PC-MoA and (d) UiO-66-PC-MoD.

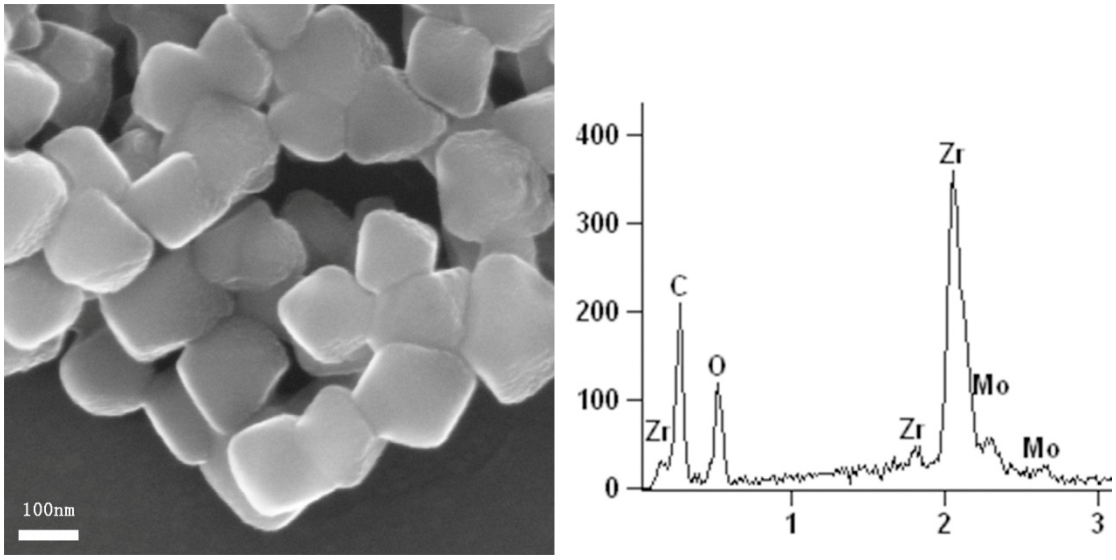

Fig S16.SEM images and EDX of UiO-66-PI-MoA.

TEM

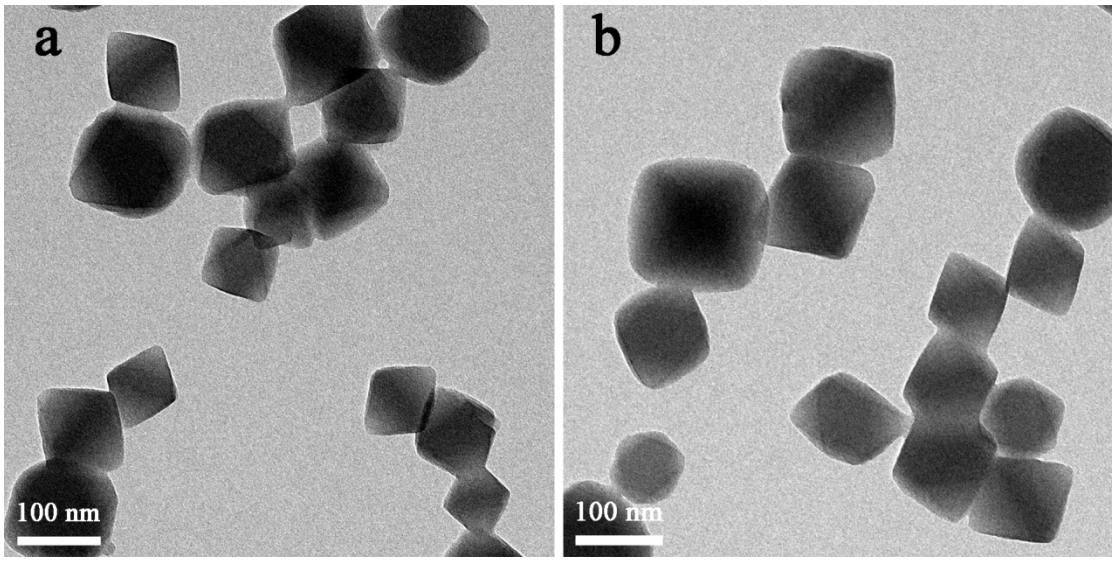

Fig S17.TEM images of UiO-66-sal-MoD: (a) fresh and (b) recovered after reaction.

References

1 K.I. Nättinen, K. Rissanen, *Cryst. Growth. Des.* 2003, **3**, 339-353.

2 H. Mimoun, IS de Roch, L. Sajus, *Bull. Soc. Chim. Fr.* 1969, **5**, 1481-1492.

3 W. Winter, C. Mark, V. Schurig, *Inorg. Chem.* 1980, **19**, 2045-2048.